Geomechanics and Engineering, *Vol. 34, No. 3 (2023) 285-301*
https://doi.org/10.12989/gae.2023.34.3.285

Probabilistic analysis of anisotropic rock slope with reinforcement measures

Zoran Berisavljević*[1], Dušan Berisavljević[1a], Miloš Marjanović[1b] and Svetlana Melentijević[2c]

[1]*Faculty of Mining and Geology, University of Belgrade, 7 Djusina Street, 11000 Belgrade, Serbia*
[2]*Faculty of Geological Science, Universidad Complutense de Madrid, c/ José Antonio Nováis 12, Ciudad Universitaria,28040 Madrid, Spain*

(*Received February 27, 2023, Revised June 19, 2023, Accepted June 29, 2023*)

Abstract. During the construction of E75 highway through Grdelica gorge in Serbia, a major failure occurred in the zone of reinforced rock slope. Excavation was performed in highly anisotropic Paleozoic schist rock formation. The reinforcement consisted of the two rows of micropile wall with pre-stressed anchors. Forces in anchors were monitored with load cells while benchmarks were installed for superficial displacement measurements. The aim of the study is to investigate possible causes of instability considering different probability distributions of the strength of discontinuities and anchor bond strength by applying different optimization techniques for finding the critical failure surface. Even though the deterministic safety factor value is close to unity, the probability of failure is governed by variability of shear strength of anisotropic planes and optimization method used for locating the critical sliding surface. The Cuckoo search technique produces higher failure probabilities compared to the others. Depending on the assigned statistical distribution of input parameters, various performance functions of the factor of safety are obtained. The probability of failure is insensitive to the variation of bond strength. Different sampling techniques should yield similar results considering that the sufficient number of safety factor evaluations is chosen to achieve converged solution.

Keywords: back-analysis; optimization technique; probability of failure; strength anisotropy

1. Introduction

Slope stability analyses are usually performed by deterministic approach (a single value is assigned to a certain soil or rock parameter), whereas the geotechnical adequacy is expressed by the factor of safety (Fs). The failure is assumed to occur when Fs is less than unity. An important limitation of deterministic approach is that slopes may have the same Fs but different probabilities of failure. This is attributed to the random and spatially variable shear strength properties. It is well known that "high" factors of safety do not necessarily mean "low" probabilities of failure (e.g., Christian *et al*. 1994, Duncan 2000).

El-Rammly *et al*. (2002) stated that: "Slope engineering is perhaps the geotechnical subject most dominated by uncertainty". Inherent spatial variability of material properties, lack of representative data, changing environmental conditions, unexpected failure mechanisms, simplifications and approximations adopted in geotechnical models and human mistakes in design and construction are all factors contributing to uncertainty. The evaluation of uncertainty can be assessed by implementation of probabilistic concepts into design. First implementation of probabilistic concept in slope engineering is attributed to the work by Wu and Kraft (1970). During the last few decades rock slope probabilistic analysis has been introduced into geotechnical practice (Christian *et al.* 1994, Low *et al.* 1998, Low *et al.* 2007, Li *et al.* 2009, Aladejare and Akeju 2020, Chakraborty and Dey 2022).

Probabilistic concept was applied to solve different geotechnical problems in slope engineering. Zhou *et al.* (2017) used Bayesian probabilistic concept to determine the failure angle of structurally controlled instabilities. Wang *et al*. (2020) used probabilistic concept to investigate the effects of water level fluctuations on earth dam slope. Probabilistic stability assessment of an earth dam under seismic loading is presented by Guo *et al.* (2020). Zhang *et al.* (2010) presented probabilistic back-analysis concept to derive parameters as random variables.

Early work by Nguyen and Chowdhury (1985) indicated that correlations between random values of shear strength parameters (namely c and φ) can influence probability of failure (P_f). These correlations are quantified by the cross-correlation coefficient (ρ). Negative cross-correlation between c and φ have been reported in literature (Lumb, 1970, Yucemen *et al.* 1973, Forrest and Orr 2010) being computed when the cohesion decreases with increasing friction angle. Javankhoshdel and Bathurst (2016) investigated an influence of cross-correlation between c and φ on numerical outcomes of simple unreinforced slopes. To our knowledge the correlation between JRC and JCS parameters of the Barton-Bandis (BB) criterion does not exist (Berisavljević *et al*. 2022), thus the influence of cross-correlation on the P_f is not of major concern when dealing with the parameters of the BB criterion.

∗Corresponding author, Professor
E-mail: zoran.berisavljevic@rgf.bg.ac.rs
[a]Professor
[b]Professor
[c]Professor

ISSN: 2005-307X (Print), 2092-6219 (Online)

Nowadays, very populistic application of probabilistic concept is in the field of random finite element method (RFEM) (e.g., Griffiths and Fenton 2004, Fenton and Griffiths 2008, Johari and Gholampour, 2018, Huang *et al*. 2010). This method combines the random field theory (RFT) with the finite element method to generate random fields of different soil/rock properties, which are then used in slope stability calculations. Probabilistic slope stability analysis performed with limit equilibrium method (LEM) by considering spatial variability of soil/rock properties is termed random limit equilibrium method (RLEM). RLEM was applied in several studies (e.g., by Li and Lumb 1987, Babu and Mukesh 2004, Ji *et al.* 2012, Javankhoshdel and Bathurst 2014, Javankhoshdel *et al*. 2017, Cho 2007).

Rafiei Renani *et al.* (2019) used probabilistic numerical analysis to explore the effect of strength variability on uniaxial compressive strength of large heterogeneous samples. It was shown that mean large-scale strength decreases with increasing small-scale variability. They extended their research to the entire slope with the conclusion that increasing strength variability leads to a reduction in mean Fs and increase in the P_f.

Wang *et al*. (2013) performed probabilistic back analysis of failure of a slope reinforced with anchors. Authors used Markov Chain Monte-Carlo technique (MCMC) and maximum likelihood method to determine the P_f of wedge-like failure using prior and posterior information on anchor force and angle of shear resistance values. The results showed that the P_f in back-analysis for updated parameters was 17.3%.

Stochastic analysis of the soil nail wall has been performed by several researchers (Javankhoshdel *et al*. 2019, Johari *et al*. 2020). Kitch (1994) performed probabilistic analysis of two reinforced slopes by LEM.

Yang and Liu (2018) used limit analysis to evaluate probability of failure of a three-dimensional rock slope.

Li *et al.* (2022) used Kriging metamodel (machine learning method) to estimate slope reliability.

Gholampour and Johari (2019) investigated an influence of unsaturated conditions (suction stress) on the reliability of braced excavation. One of the main conclusions implies that the standard deviation and mean value of lateral wall deflection and bending moment decreases significantly if suction is introduced.

Johari *et al.* (2013) introduced the Jointly Distributed Random Variables method for probabilistic analysis of rock slope with planar slip surface.

Probabilistic and statistical concepts are implemented in Eurocodes (in particular Eurocode 7 - European standard for geotechnical design), where, for example, representative values of geotechnical parameters may be determined by statistical procedures (Tietje *et al*. 2014). Ray and Baidya (2014) used reliability-based approach to determine partial factors for different random variables of a slope under static loading conditions.

Probabilistic LEM slope stability analysis (along with RLEM) could be readily performed in commercially available software such as Slide2 version 9.020 (RocScience, 2021). Software offers the ability to assign cross-correlation between various geotechnical parameters, different probability distribution functions along with different probabilistic sampling techniques (such as Monte-Carlo - MC; Latin-Hypercube - LHC, McKay *et al.* 1979, or Response surface, Box and Wilson 1951) to search for the probability of failure (P_f) or reliability index (RI). In order to find the critical sliding surface there are two optimization techniques available in Slide2 software, namely Monte-Carlo random walk (Greco 1996) and Surface Altering - local optimization technique. Surface Altering optimization is recommended as it is faster than Monte-Carlo and able to find more critical surfaces (Javankhoshdel *et al.* 2018).

These techniques could be combined with the global non-circular search methods such as: Block Search, Path Search, Simulated Annealing, Auto Refine and Cuckoo to obtain even lower safety factor values of non-circular slip surfaces (RocScience 2022). The combination of these optimization techniques is used throughout the analysis process of the studied slope presented in this paper. Another efficient and robust way to determine the position of the critical failure surface is the usage of the hybrid genetic algorithms (e.g., Li *et al*. 2009).

The aim of this study is to investigate the capabilities of probabilistic forward analysis to predict the failure of reinforced cut slope in anisotropic rock mass (incorporating uncertainties in shear strength parameters of adversely oriented discontinuities and anchor bond strength). It is worth mentioning that the uncertainty in shear strength of discontinuities is described by the variability of Barton-Bandis parameters, instead of routinely applied Mohr-Coulomb parameters. The particular focus is placed on the investigation of the influence of various optimization techniques (for searching the critical sliding surface) on the overall probability of failure of a marginally stable slope with complex reinforcement measures.

2. Basic probability concepts

Reliability analysis is concerned with finding the reliability (R) or the probability of failure (P_f) of a certain feature that governs the problem at hand. The term Reliability R should not be misused with the term Reliability Index that will be defined in the following. In order to make a difference between the designation of beta distribution and reliability index we will use abbreviation RI for reliability index throughout the study. Reliability and probability of failure sum to unity and are expressed as

$$R + P_f = 1 \tag{1}$$

To distinguish adverse but non catastrophic events from events of catastrophic failure, the term probability of unsatisfactory performance P_u is sometimes used (US Army Corps of Engineers 1997).

Influencing parameters that have a significant uncertainty in the design of different geotechnical problems (i.e., shear strength parameters c, φ) are taken as random variables. Instead of having precise single values, random variables assume a range of values in accordance with a probability density function (PDF) or probability distribution, which quantifies the likelihood that its value lies in any given interval.

If one could define the probability density function $f_x(x)$,

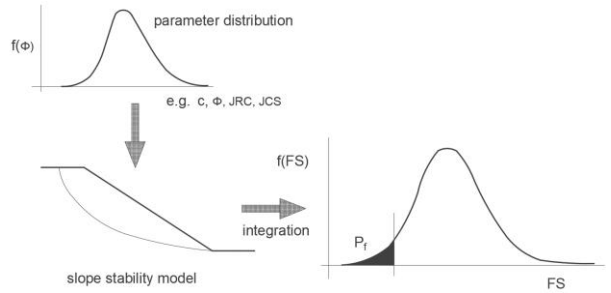

Fig. 1 Definition of performance function and probability of failure in slope stability analysis (modified after Wolf, 1996)

for each random variable x_i, in a slope stability analysis, then one could, construct the PDF for the factor of safety $f(F_s)$. The PDF function defined for the factor of safety value is termed performance function. If the limit state is taken as the condition Fs=1, then the area of PDF below the limit state is the P_f. These concepts are illustrated in Fig. 1.

two groups: approximate methods (the FOSM method, the point estimate method) and Monte-Carlo simulation (MCS).

Besides these two methods, several advanced methods have been developed with the aid of artificial intelligence techniques (e.g., Zhang *et al*. 2023, Wang *et al.* 2020). Approximate methods allow the estimation of the mean value and variance of the factor of safety. These methods, however, do not provide any information regarding the shape of the probability density function. The failure probability can only be obtained by ascribing the probability distribution function to the factor of safety.

Depending on the amount of data at hand, different approaches can be adopted to estimate the probability distribution of each input variable. For the large number of data (e.g., many shear test results for assessing *c* and φ values), the cumulative distribution function (*CDF*) of the measurements can be used in the slope stability analysis. If only a few data exist, parametric distributions can be assumed from the literature. The coefficients of variation and probability density functions of various soil properties have been presented in different studies (e.g., Lumb 1966, Harr 1987, Kulhawy *et al.* 1991, Lacasse and Nadim 1996).

Selected distributions of the input parameters should be limited by the physical range of the parameter involved. For example, shear strength parameters never take negative values. If the selected distribution extends towards negative values, it should be "cut-off" to a practical minimum threshold.

Monte-Carlo simulation is based on the generation of random numbers, which are used in sampling the cumulative distribution function of the input variables. The result of a Monte-Carlo simulation depends on the number of iterations. With sufficient number of iterations, the *CDF* obtained by sampling should closely match the original input *CDF*. Large number of iterations produce stable and consistent solution at the expense of increasing computational time. The optimum number of iterations mostly depends on the level of the uncertainties in the input parameters, correlation among them and the type of output parameter. In order to optimize the simulation process, the analysis could be repeated several times using the same seed value and an increasing number of iterations. A plot of the number of iterations against the probability of failure indicates the minimum number of iterations at which the probability reaches a constant value. The output of the MCS is the probability density function of the factor of safety.

The probability of failure is obtained as the number of iterations with $F_S < 1.0$, relative to the total number of iterations.

Because the simulation process uses random sampling of the input variables, the calculated probability of failure is also a variable, meaning it could differ from one to another simulation process. Law and McComas (1986) concluded that relying on the results of a single simulation run is one of the most common and potentially dangerous simulation practices. The simulations should be repeated many times using different seed values to assess the consistency of the estimates. In this way the histogram of the probability of unsatisfactory performance, the mean probability, and the 95% confidence interval around the mean value could also be estimated (El-Ramly *et al.* 2002). Due to practical limitations related to the large computational times the constant seed value is used throughout the simulation process in this study.

Important equations, terms and definitions related to the probabilistic theory are given in tabular form (Table 1).
Another important parameter used to express the failure probability is reliability index (RI) and is given by

$$RI = \frac{\bar{x}\,[Fs]-1}{s[Fs]} \tag{2}$$

where $\bar{x}[F_S]$ and $s[F_S]$ are the mean and standard deviation of the F_S, respectively. The above definition is applicable if the performance function (factor of safety equation) is linear, which is not the case for slope stability models. Mostyn and Li (1993) suggested that the performance functions of slopes are reasonably linear and recommended ignoring the nonlinearity when calculating RI. Christian *et al.* (1994) stated that the abovementioned definition does not require that the probability distribution of F_s be known, but there is a tacit assumption that the F_S is distributed in some way that can be described meaningfully by an expected value and standard deviation. Table 2 shows reliability indices that should be used as general guidelines. Acceptable values of RI in slope engineering range between 2 and 3 ($0{,}1\% < P_f < 2.3\%$), defined in terms of expected performance level between above average and poor. In certain cases, and depending on the application, the admissible P_f could be even higher than 3%.

As mentioned earlier, the Monte-Carlo simulation is dependent on the number of samples. Robert and Casella (2004) stated that the number of samples during Monte-Carlo simulation should be at least 10 times higher than the inverse value of the probability of failure in order to obtain reliable result.

For any slope, there is an unlimited number of potential slip surfaces. The slope may fail along any of these surfaces. The total probability of failure is accounted only

Table 1 Basic descriptive statistics terms and probability functions used in study

Equation	Definition	Note
$\bar{x} = \frac{\sum_{i=1}^{n} x_i}{n}$	$\bar{x}$ - *mean value* of a set of n measured values for the random variable x	(in units of random variable)
$s = \sqrt{\frac{\sum_{i=1}^{n}[(x_i-\bar{x})^2]}{n-1}}$	s - *standard deviation*; s^2 - *variance* is the second central moment	The standard deviation measures the dispersion of a dataset relative to its mean value. The value s is usually called the empirical standard deviation, or the corrected standard deviation in order to distinguish it from the standard deviation of the population. The reason that n -1 appears instead of n in the denominator is that the mean is also an estimated value, so the number of degrees of freedom has to be decreased by one (BESSEL'S correction). (in units of random variable)
$V = \frac{s}{\bar{x}} \cdot 100\%$	V - *coefficient of variation*	To provide a convenient dimensionless expression of the uncertainty inherent in a random variable, the standard deviation is divided by the expected value to obtain the coefficient of variation which is usually expressed as a percent
$C_s = \frac{n\sum_{i=1}^{n}(x_i-\bar{x})^3}{(n-1)(n-2)s^3}$	C_s - *coefficient of skewness* is the quotient of the third central moment and the standard deviation raised to the third power.	Skewness is a measure of the asymmetry of a distribution. The coefficient of skewness unlike the standard deviation is a quantity with a sign, since the sum appearing in the numerator of expression may be either positive or negative. Consequently, the signed value of C_s is the index of the direction and the magnitude of the asymmetry. If $C_s > 0$, the density function is extended toward larger numbers and vice versa. As the differences x_i-x appear to the third power, the coefficient of skewness is very sensitive to the outlying (extreme) values. Calculating the coefficient of skewness for small samples must be accepted with reservation (also valid for kurtosis)
$C_k = \frac{n\sum_{i=1}^{n}(x_i-\bar{x})^4}{(n-1)(n-2)s^4} - 3$	C_k - *Kurtosis* is the quotient of the fourth central moment by the fourth power of the standard deviation minus 3	The kurtosis is the index of the "peaked" nature of the distribution: if $C_k > 0$, then the central section of the density function is higher than in a normal distribution and vice versa. The additive term (-3) in expression reflects the fact that for the normal distribution the value of the fraction is 3. Coefficient of skewness is very sensitive to the extreme values.
$K=\frac{\beta_1(\beta_2+3)^2}{4(2\beta_2-3\beta_1-6)(4\beta_2-3\beta_1)}$	K - *value defining Pearson's criterion*	where, β_1 characterizing the skewness and β_2 characterizing the peakidness may be calculated from the following expressions: $\beta_1=C_s^2$ and $\beta_2=C_k+3$
$f_x(x)=\frac{1}{x_{is}\sqrt{2\pi}} e^{-\frac{(x-\bar{x})^2}{2s^2}}$ $-\infty<x<\infty$	*Normal distribution*	
$f_x(x)=\frac{(b-a)^{-1-\alpha-\beta}}{B(\alpha+1,\beta+1)}(x-a)^{\alpha}b-x^{\beta}$ $a\leq x\leq b,\ \beta>-1,\ \alpha>-1$	*Beta distribution, Euler-type beta-function:* $B(\alpha+1,\beta+1)=\frac{\Gamma(\alpha+1)\Gamma(\beta+1)}{\Gamma(\alpha+\beta+2)}$, Γ - *Gamma-function*	The parameters α and β may be determined as follows: $\alpha=\frac{x_r^2}{V_r}(1-x_r)-(1+x_r)$, $\beta=\frac{\alpha+1}{x_r}-(\alpha+2)$, *where* $x_r=\frac{\bar{x}-a}{b-a}$, $V_r=(\frac{s}{b-a})^2$, a, b *- extreme values of analysed dataset*

for the admissible slip surfaces. These surfaces, however, are highly correlated, since they are all analyzed using the same input variables and the same analytical model.

Hassan and Wolff (1999) indicated the difference between the deterministic critical slip surface and the most critical probabilistic slip surface. They have proposed a search algorithm for locating the slip circle with the minimum reliability index.

3. Engineering background

In the recent study by Berisavljević *et al*. (2022) a detailed description of geological conditions of the Paleozoic schist rock mass, that is the base rock of the highway E75 passing through Grdelica gorge, was presented. Within the framework of the present study, it is important to emphasize the anisotropic nature of the schist with adversely oriented discontinuities dipping towards the excavation.

Overall geotechnical properties of the schist depend on the weathering grade and tectonic disturbance of the rock mass. In the more competent rock failures are usually structurally controlled, i.e., formed along the adversely oriented joints.

In the weathered units the deep-seated failures are formed. Geological map of the wider area, with locations of rock cuttings that have suffered from different kind of instabilities, due to complex geological conditions and construction requirements, is shown on Fig. 2.

This study presents the analysis of the failure of cut no. 2, that occurred in August 2018, Fig. 3. The implemented design solution in the zone of cut no. 2 consisted of two rows of micropile walls with prestressed anchors. The

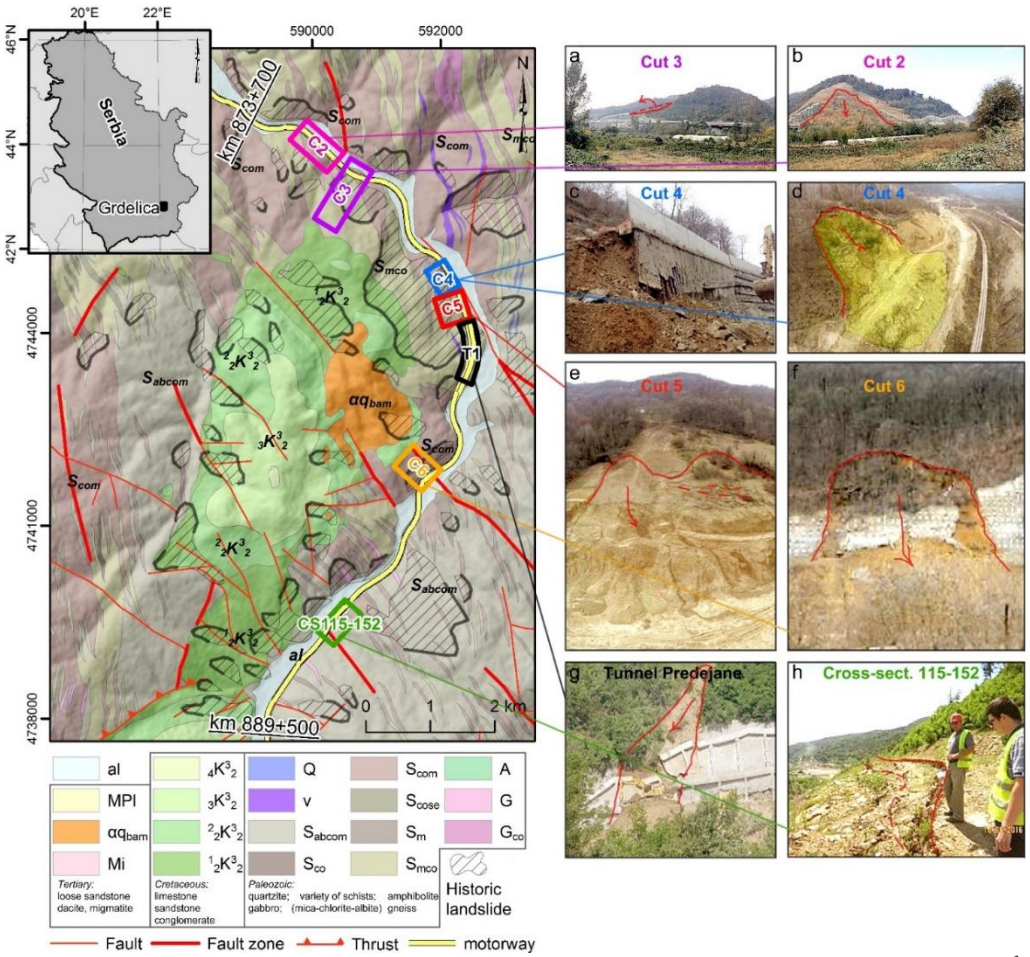

Legend symbols: al – alluvial deposits (Quaternary); MPl – Miocene-Pliocene clastites (Tertiary); αq_{bam} – dacite (Tertiary); Mi – migmatite (Tertiary); $_4K_2^3$ & $_3K_2^3$ – limestone (Cretaceous); $_2K_2^3$ – sandstone (Cretaceous); $_1K_2^3$ –conglomerate (Cretaceous); Q – quartzite (Paleozoic); v – gabbro (Paleozoic); S_{abcom} S_{mno} – variety of schists with alternating content of mica, chlorite and albite components (Paleozoic); A – amphibolite; G & G_{co} – gneiss (Paleozoic)

(a) Failure of cut no. 3, (b) failure of cut no. 2, (c) local failure of micropiles in the zone of cut no. 4 at km 879+125, (d) global failure in the zone of cut no. 4, (e) failure of cut no. 5, (f) failure of reinforced slope in the zone of cut no. 6, (g) failure in the zone of exit portal slope of tunnel Predajane, (h) structurally controlled failure between cross sections CS 112 and CS 152

Fig. 2 Simplified geological map of the area under study with location of cuttings that have undergone different kind of instabilities

Table 2 Target reliability indices (US Army Corps of Engineers, 1997)

Expected Performance Level	Reliability index RI	Probability of Unsatisfactory Performance
High	5	0.0000003
Good	4	0.00003
Above average	3	0.001
Below average	2.5	0.006
Poor	2	0.023
Unsatisfactory	1.5	0.07
Hazardous	1	0.16

Table 3 Characteristics of prestressed anchors

Steel class	Y 1770 S7
Strand diameter (mm)	15.3
No. of strands per one anchor	5
Cross-sectional area of one strand (mm^2)	140
Tensile strength (N/mm^2)	1770
Characteristic breaking force of one strand / force at permanent strain of 0.1%	248 / 218
Overall anchor length L / bond length L_b (m)	25-30 / 15
Prestressing force (kN)	450

micropiles were constructed using high quality seamless steel (f_u=550 MPa, where, f_u - tensile strength of steel) tubes d_{int}/d_{out} = 122 mm/139.6 mm (d_{int}, d_{out} -internal and external diameter, respectively). The hollow tubes were filled with concrete C25/30 from the inner and outer side to form a micropile with 200 mm in diameter. The axial spacing between micropiles is 1.5 m. The length of micropiles varied between 22 and 26 m. Depending on the geological profile and the height of the cutting, one or several rows of micropile wall were constructed. The ultimate (non-factored) micropile shear strength of 397 kN is used in back analysis by limit equilibrium slope stability method.

Permanent prestressed anchors were installed in boreholes of 131 mm diameter. The anchor load is

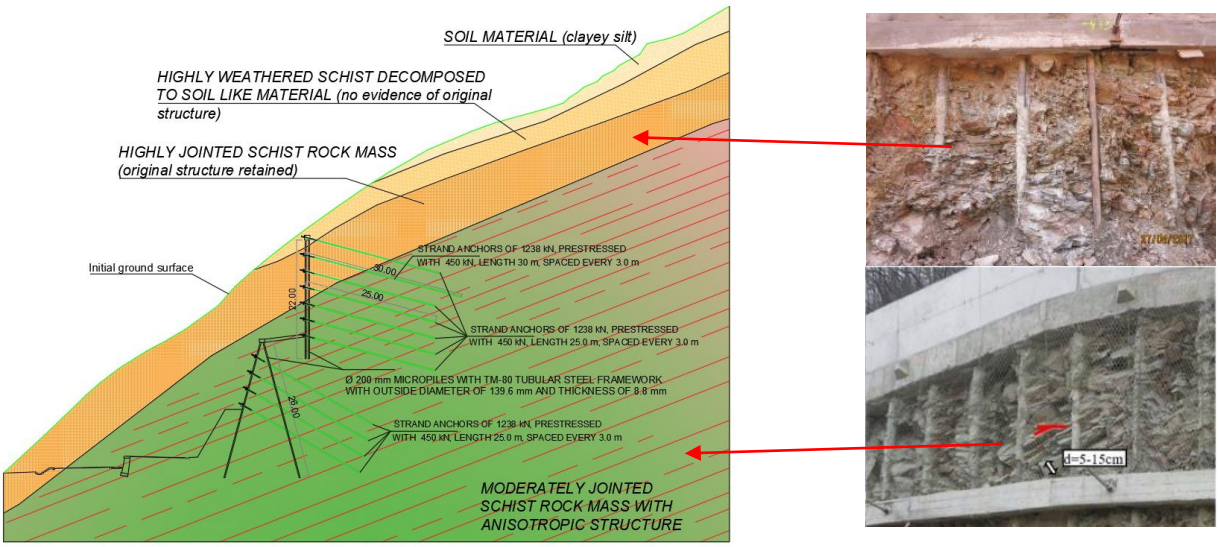

(a) Geometry of cross-section 876+150 excavated in highly and moderately jointed schist rock mass

(b) View of one portion of reinforced slope

(c) Close-up of a load cell

(d) Failure of cut no. 2 in August 2018 (orange line indicates position of cross-section 876+150)

Fig. 3 Implemented structural measures prior to the failure and failure of cut no. 2

transferred to the tie beam (steel class S235) over the galvanized steel plate. The anchors characteristics are shown in Table 3.

The characteristic breaking force of the anchor with five strands is $R_{p,k}$=1239 kN; Design anchor resistance: ($R_{t,d}$)= $R_{p,k}/\gamma_a$ = 918 kN, where γ_a - partial factor of 1.35 (according to EN1537, 2013). Considering that the study focuses on the back analysis of rock mass failure, the anchor characteristic breaking force $R_{p,k}$ was used throughout this study (and not the design resistance).

The excavation was executed in stages. At first, micropiles were installed within the rotary-percussion drilled boreholes. After curing of concrete around and within the steel micropile tubes vertical excavation was executed. Each excavation stage was 4.0 m deep.

All reinforcing measures (installation of anchors, construction of anchor tie beam and prestressing of anchors) were applied prior to the excavation of subsequent vertical

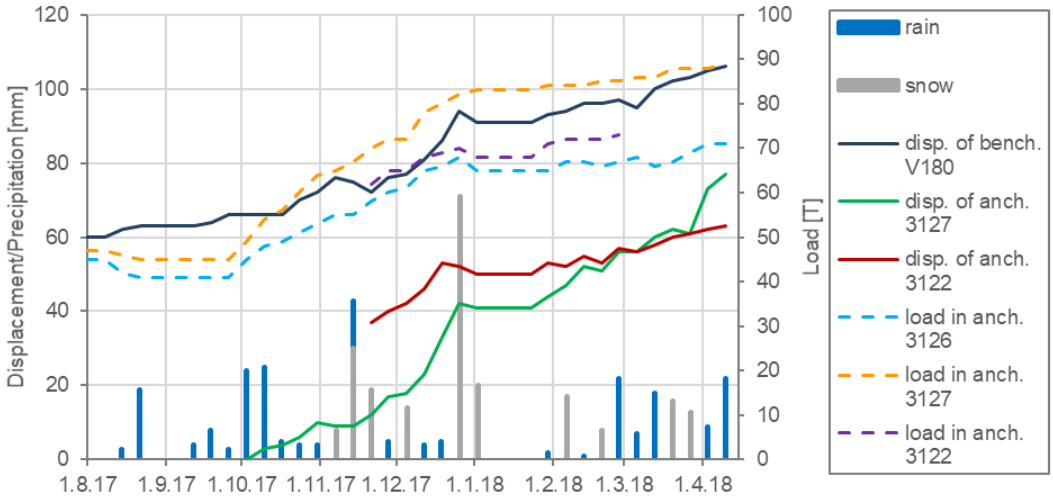

(a) Precipitation, load and displacement vs time (loads are given for several anchors (measured with load cells in dashed lines, while displacements are in solid, as well as overall displacement for geodetic benchmark V180 installed in the zone of failed section)

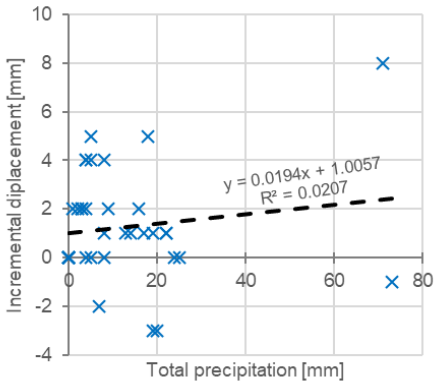

(b) Correlation of incremental overall displacement for benchmark V180 vs total (rain and snow) daily precipitation

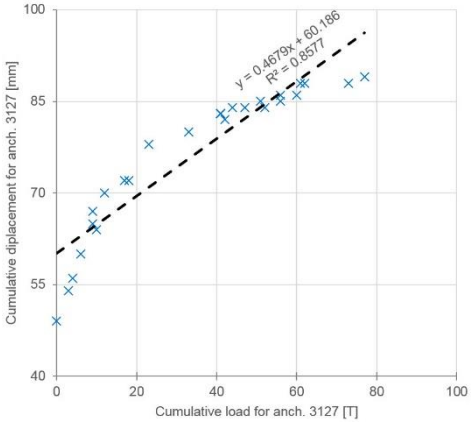

(c) Correlation between cumulative displacement vs. load for anchor 3127

Fig. 4 Monitoring results

stage. Abovementioned operations continued until reaching the final depth. In the zone of the deepest excavation the concrete berm (3 m wide) and additional row of inclined micropiles were constructed, Fig. 3(a). Typical representatives of highly and moderately jointed schist rock mass are also shown in Fig. 3(a). The uppermost portion of schist is completely decomposed to soil like material with colluvial clayey silt above it.

The view of finished wall face (sprayed with shotcrete) and drainage holes are shown in Fig. 3(b).

Fig. 4(a) shows the load (dashed) and displacement (solid) curves of several anchors over time, on the same timeline with precipitation (vertical bars). The force in anchors was measured with load-cells (refer to Fig. 3(c) for details).

Precipitation in form of rain and snow events are shown as light blue and light gray bars, respectively. Green and dark red solid lines show displacement of anchors 3127, 3122, while overall displacement, related to benchmark V180 and in vicinity of anchor 3126 is given in dark blue.

Load and displacement curves generally show constant trend till October 2017. Afterwards, the gradual increase of load and displacement was observed until failure occurred in August 2018. The shift of displacement curve of anchor 3122 (not starting from nil) is a consequence of the addition of the overall structure displacement measured in its vicinity. There is no tangible correlation of incremental displacements vs. total precipitation (rain and snow), wherein even for a very small or no precipitation displacements were apparent (Fig. 4(b)). Only intensive snowing (and probably thawing) events occurring at the end of 2017 and beginning of 2018 have strong response in displacement, equaling up to 8 mm. On the other hand, cumulative displacement is in line with increasing load in cells (Fig. 4(c)), wherein positive correlation trend is slightly sloping, meaning that load increment step is higher than displacement increment step (loads increase more than displacement over time). Such a trend might indicate slight yielding of anchoring elements which is pronounced in the beginning but decreases with time, as secondary load settles

(a) Prestressing of anchors with a multi-jack

(b) Preparation works for connecting micropiles with capping beam

(c) View of the failed section after removal of unstable material and slope rearrangement

(d) Gallery as a remedial measure

Fig. 5 Construction activity over time

over time. Fig. 3(d) shows the extent of failure and position of the cross-section 876+150.

Construction activity is shown on Fig. 5. The gallery founded on piles was constructed as the final remedial measure, Fig. 5(d).

4. Assessment of schist rock mass strength parameters

Obtained parameters, as shown in Table 4, are the result of comprehensive site investigations during the design stage. For soil material and highly weathered and decomposed schist rock mass, parameters were determined directly in soil mechanics laboratory (mainly by means of direct shear tests on undisturbed samples). Three samples per direct shear test

(up to 300 kPa of normal stress level) were tested. Resistance parameters (c and φ) were determined as characteristic values (from the mean value of n sample derived values) of the ground property according to the procedure proposed by Eurocode 7. The coefficient of variation V(%) was determined for the case where V is "unknown" ab initio.

The rock mass parameters of highly and moderately jointed schist rock mass were determined according to the Hoek-Brown failure criterion (Hoek *et al*. 2002, Hoek and Brown 2019). Detailed engineering geological mapping, along with the laboratory testing, produced the best estimated parameters of the Hoek-Brown (HB) failure criterion. During the design process, equivalent Mohr-Coulomb parameters were determined for the dimensioning of the retaining structure. However, in this study HB parameters were applied directly to the rock mass in order to avoid stress dependent misconceptions that are common for the linear MC parameters (e.g., Rafiei Renani and Martin 2020). While for the highly jointed schist rock mass HB assumption regarding isotropic behavior is valid, for moderately jointed schist the strength anisotropy had to be considered. Due to the "ubiquitous" nature of unfavorably oriented joints (refer to Fig. 3(a)) directional model was introduced into the slope stability analysis. Joint orientations were collected for 481 data in the zone of cut no. 2. These data are reproduced on stereographic projection (Fig. 6a) that also shows cut face orientation along with the mean orientation of critical (unfavorably oriented) joint set. These joints are spaced on average between 5 and 15 cm. The critical joint orientation has the same dip direction as that of the slope (daylighting at the slope face), thus producing conditions for application of directional models.

Throughout the analysis, the generalized anisotropic model was used, for which the value of shear strength depends on the angle between the slice base and discontinuity dip angle. The angular range (from the hypothetical horizontal line) for which the joint strength parameters should be applied at the base of the slice varied between 45° and 60° (Fig. 6(b)). This range is the measured variation of the critical joint dip angle towards the slope. Critical joints are persistent, smooth to slightly rough and moderately weathered. Soft (low plastic clays and silts) and hard (quartz veins) infill is usually present in other joint sets, whereas critical joint set is without infill. In terms of material parameters Barton-Bandis criterion (Barton 1973,

Table 4 Values of shear strength parameters of different units (see Fig. 3(a))

	HB criterion $\sigma_1=\sigma_3+\sigma_{ci}(m_b\sigma_3/\sigma_{ci}+s)^a$	Mohr-Coulomb criterion $\tau=c+\sigma_n\tan\varphi$	BB criterion $\tau=\sigma_n\tan\left[JRC\cdot\log_{10}\left(\frac{JCS}{\sigma_n}\right)+\varphi_r\right]$
Soil material		γ=19 kN/m^3; c=15 kPa; φ=27°	
Highly weathered schist (soil like material)		γ=22 kN/m^3; c=15 kPa; φ=27°	
Highly jointed schist rock mass	γ=25 kN/m^3; σci=12 MPa; GSI=20; mi=7;		
Moderately jointed schist with adversely oriented joints	γ=26 kN/m^3; σ_{ci}=45 MPa GSI=40; mi=10;		JCS=29.7-61.5 MPa; JRC=3-11 φ_r=21°

Table 5 Descriptive Statistics of BB parameters

	JRC	JCS
No. of data (n)	23	23
Mean	6.348	45.803 MPa
Median	6.000	49.980 MPa
Std. Deviation	2.014	11.182 MPa
Skewness	0.719	-0.098
Std. Error of Skewness	0.481	0.481
Z value (Skewness)	1.494	0.204
Kurtosis	0.055	-1.473
Std. Error of Kurtosis	0.935	0.935
Z value (Kurtosis)	0.059	1.575
Shapiro-Wilk	0.933	0.907
P-value of Shapiro-Wilk	0.128	0.035
Minimum	3.000	29.710 MPa
Maximum	11.000	61.530 MPa

1976, Barton and Choubey 1977, Zhao *et al*. 2020) is applied. Details on joint parameter derivation is shown in the study by Berisavljević *et al*. (2022).

5. Probabilistic assessment of joint parameters

Twenty-three paired measurements of JRC and JCS values were obtained on different joints within the critical joint set. The results of descriptive statistics of measured data were obtained in open-source statistical software JASP and results are reproduced in Table 5.

The value of residual friction angle for critical joint set was determined as φ=21° (Berisavljević *et al*. 2022).

The common assumption when dealing with probability in geotechnical engineering is to assume that the variation of material properties is described by normal distribution function. This assumption is usually valid for large data sets. However, in certain cases one could try to determine which distribution function best describes the data at hand.

For the analyzed dataset (JRC and JCS values) Shapiro-Wilk test (Shapiro and Wilk 1965) was performed in order to check if the variables are following normal distribution.

Table 6. Parameters of the Pearson's system for JCS and JRC variables

	JCS	JRC
n (no. of samples in a population)	23	23
$\bar{x}$	45.803	6.347
s	11.181	2.013
C_s	-0.098	0.719
C_k	-1.346	-0.073
$\beta_1 = C_s^2$	0.0097	0.517
$\beta_2=C_k+3$	1.653	2.927
"K" value	-0.0029	-0.263
x_r	0.506	0.418
V_r	0.123	0.063
α	-0.482	0.188
β	-0.493	0.652
$\bar{x}$ (expected value of beta distribution)	45.803	6.348
s^2 (variance of beta distribution)	125.035	4.055

As a rule of thumb, if P-value (probability) of Shapiro-Wilk test is less than 0.05, the null hypothesis (that the variable is normally distributed) could be rejected. The results of Shapiro-Wilk test show that the normality assumption is violated for JCS value, while for the JRC value the data could be normally distributed. Having in mind that normality tests have low power in small sample sizes, the method of assessing normality using skewness and kurtosis (the z-test) of the distribution (Kim 2013) was used to check the normality assumption. A z-score is obtained by dividing the skew values or kurtosis by their standard errors

$$Z = \frac{Skewness}{Std.\ Error\ of\ Skewness}, Z = \frac{Kurtosis}{Std.\ Error\ of\ Kurtosis} \quad (2)$$

For small samples (n<50), if absolute z-scores for either skewness or kurtosis are larger than 1.96 (which corresponds to P-value of 0.05) the null hypothesis should be rejected (Kim 2013).

As shown in Table 5, the z-values for both skewness and kurtosis of JRC and JCS are far below the value of 1.96 implying that the analyzed data is normally distributed.

The discrepancy between the Shapiro-Wilk and z-score tests are obvious for analyzed JCS values. Due to this reason the Pearson's system (Pearson 1916) of statistical distributions is used to determine the exact form of analyzed distributions. Pearson's system distinguishes seven types of curves (I-VII), depending on the value of the so-called "K" criterion. The detailed procedure of determining the "K" value and β_1 and β_2 parameters is shown by Rethati (1988). The relevant equations are summarized in Table 1.

If represented by dots on Fig. 7, JRC and JCS variables belong to the β-distribution (I.). The JCS variable is best described by "U" shaped β-distribution for which α and β are both negative, Table 6. The JRC variable could be described by the "bell-shaped" β-function (for which α and β have the same sign).

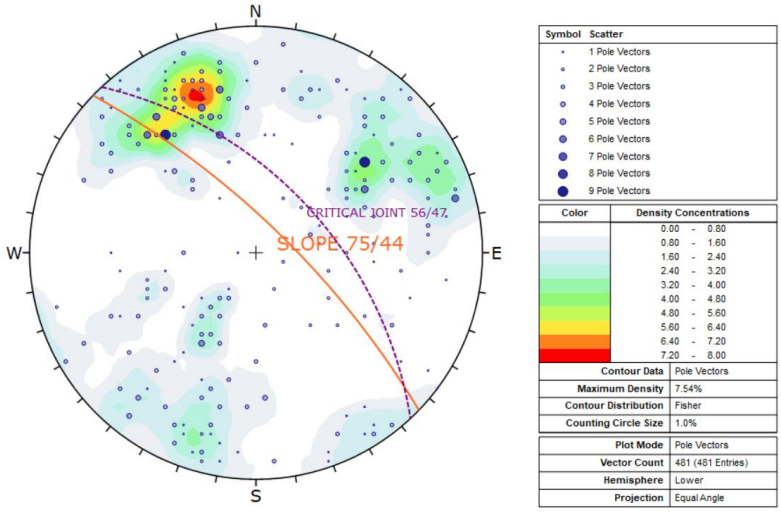

(a) Pole plot of discontinuities in the zone of Cut no. 2

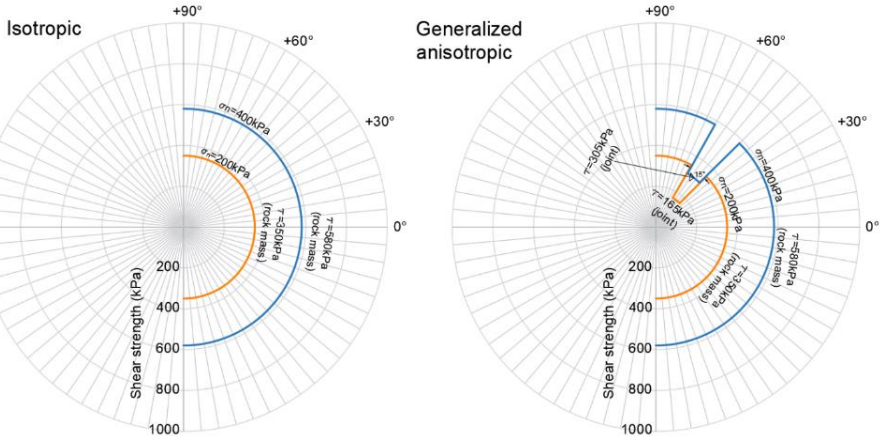

(b) schematic representation of isotropic and anisotropic strength parameters of schist rock mass in the zone of cut no. 2 (modified after Berisavljević *et al.* 2019)

Fig. 6 Orientation of joints and strength anisotropy

6. Variation in the anchor bond strength

Along with the shear strength parameters of critical joint set the statistical distribution is assigned to the bond strength value of anchor system. This is done in order to account for the rock mass variability in the anchor bond zone. Steel properties are well-known thus the material variability is not considered. Anchor bond strength in the zone of moderately weathered schist rock mass is determined as a fraction of rock mass strength (σ_{rm}). According to the BS 8081:2015+A2:2018 (Code of practice for grouted anchors) for rocks with the absence of shear strength data or field pull–out tests, the ultimate skin friction may be taken as 10% of the unconfined compressive strength of the rock mass (σ_{rm}). In this case the σ_{rm} equals 6425 kPa, thus the anchor bond resistance $R_{e,k,1m}$ equals 264 kN/m'. The variation is accounted for by assuming that $R_{e,k,1m}$ represents the mean value, while the standard deviation is obtained by introducing the coefficient of variation of V=20%, corresponding to the proposed value of coefficient of variation for the shear strength at failure in Eurocode 7 (EN 1997-1:202x) standard (V=15 - 25%).

7. Results of analyses

Deterministic and probabilistic slope stability analyses are performed by means of the limit equilibrium method in software Slide2 (RocScience, inc.). Cross-section CH 876+150 (refer to Fig. 3) was analyzed under the assumption of plane strain conditions. Spenser's method (Spenser 1967) that satisfies all conditions of static equilibrium was used throughout the analysis. Circular sliding surface is considered for deterministic analysis, while both circular and non-circular (composite) sliding surfaces are considered within the probabilistic analysis.

Deterministic approach was considered for isotropic and anisotropic case. For isotropic case critical joint set is excluded from the analyses and only rock mass parameters are considered. The safety factor value is well above the critical value (F_s=1.0) and it depends on the type of search technique. Critical sliding surface (with the lowest F_s) is positioned in the upper part of the slope (above the upper row of micropiles), Fig. 8. This position remains approximately the same for all isotropic cases analyzed.

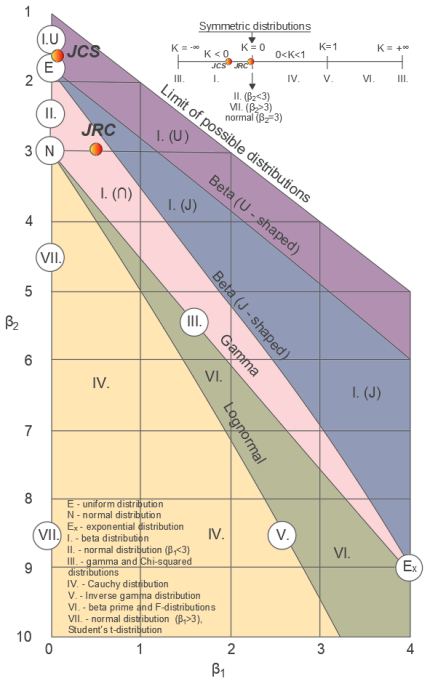

Fig. 7 Pearson's system of statistical distribution functions in β1, β2 coordinate system (note the "K" criterion scale is shown in the upper right corner of Fig. 7) (modified after Rethati 1988)

Table 7 Results of deterministic analyses

* Fs (deter.)	Circular surfaces		Non-circular surfaces with optimization		
	Slope search	Auto Refine search	Path search	Cuckoo search	Particle swarm search
Isotropic	1.357	1.286	1.357	1.266	1.271
Anisotropic	1.204	1.076	1.103	1.046	1.013

In the case of anisotropic analyses safety factor values are close to unity, except for the *Slope search technique* for which Fs=1.204. Critical sliding surfaces are positioned in the upper portion of the slope and their shape corresponds to the failure surface observed on site (refer to Fig. 3), Fig. 8. Results of deterministic analyses are shown in Table 7.

Two sets of probabilistic analyses are performed to inspect whether different types of statistical distributions (for describing the joint shear strength parameters) have an influence on the result. The first set of analyses considered an assumption of β-distribution of input variables JRC and JCS and normal distribution for anchor bond strength. In the second set of analyses normal distribution was assigned to the input variables. Multiple analyses are performed for each scenario by varying sampling method (MC or LHC simulation) and the failure surface search method (for circular surfaces: Slope search and Auto refine search; for non-circular surfaces with additional optimization: Path search, Cuckoo and Particle swarm search). In order to investigate whether the bond strength has an influence on the analysis result, an additional set of calculations is performed by excluding the bond strength variability (bond strength is set equal to its mean value).

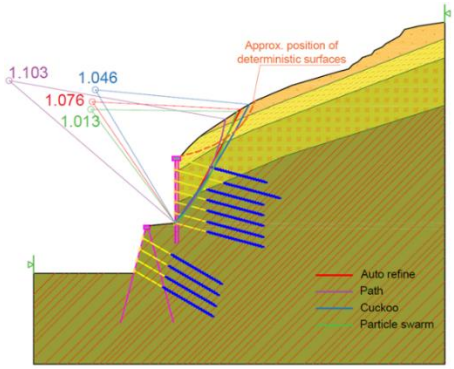

Fig. 8 Results of deterministic slope stability analyses of anisotropic rock mass for different search techniques

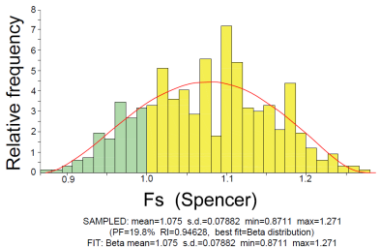

(a) Auto refine search

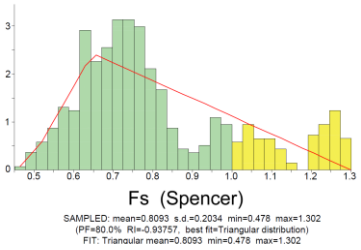

(b) Path search

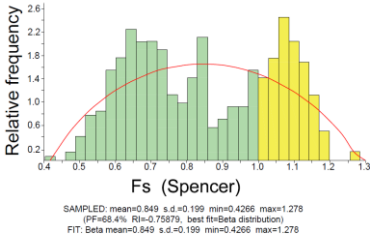

(c) Cuckoo search

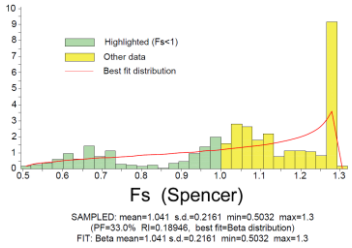

(d) Particle swarm search

Fig. 9 Performance functions of the factors of safety with β distribution prescribed to input variables JRC and JCS

The computational time for probabilistic approach is highly dependent on the number of Fs evaluations, and optimization search technique used. The x64 based-PC 11th Gen Intel(R) Core (TM)i5 processor, with 16 GB RAM, 2.4GHz, 4 core(s) and 8 logical processor(s) was used to perform analyses.

Table 8 Probability of failure with bond strength variability for different sampling and optimization techniques for β and normal distribution

β / Normal distribution	Circular surfaces		Non-circular surfaces		
	Slope search	Auto Refine search	Path search	Cuckoo search	Particle swarm search
MC (5000 evaluations)	0.0 / 0.0	19.16 / 17.48	84.12 / 86.20	66.92 / 66.30	32.30 / 33.84
LHC (500 evaluations)	0.0 / 0.0	19.80 / 17.40	80.80 / 87.20	68.40 / 66.40	33.0 / 33.40
Computation time - MC	22min / 25min	14h 59min / 15h 31min	9h 40min / 9h 32min	23h 30min / 22h 54min	20h 18min / 20h 33min
Computation time - LHC	5min / 4min	9h 12min / 8h 43min	6h 35min / 6h 40min	11h 30min / 11h 18min	9h 11min / 9h 17min

Table 9 Mean factor of safety and reliability index with bond strength variability for different sampling and optimization techniques (β distribution)

Fs(mean) / RI	Circular surfaces		Non-circular surfaces		
	Slope search	Auto Refine search	Path search	Cuckoo search	Particle swarm search
MC (5000 evaluations)	1.214 / 3.227	1.074 / 0.951	0.777 / -1.353	0.850 / -0.747	1.039 / 0.177
LHC (500 evaluations)	1.215 / 3.225	1.075 / 0.946	0.809 / -0.938	0.849 / -0.759	1.041 / 0.189

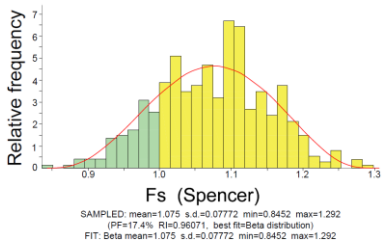

(a) Auto refine search

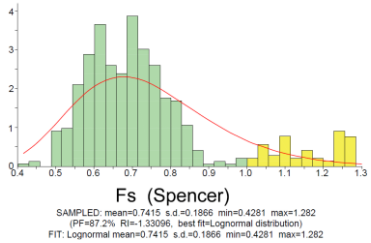

(b) Path search

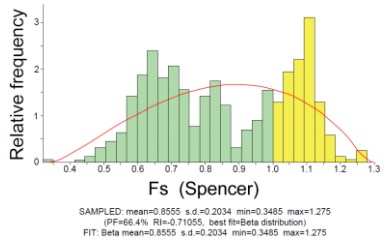

(c) Cuckoo search

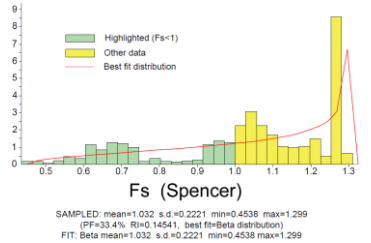

(d) Particle swarm search

Fig. 10 Performance functions of the factors of safety with normal distribution prescribed to input variables JRC and JCS

In order to determine optimal number of samples (evaluations), for which the convergence is achieved, the initial analyses were performed with 1000 samples for LHC method and 10000 samples for MC sampling method (with all other options set to default values). It was noticed that the convergence is achieved for LHC method after only 250 iterations. To make sure that the convergence is achieved in all subsequent analyses the number of samples was set to 500. For MC sampling technique convergence is achieved after 4000 iterations, thus all subsequent analyses were performed with 5000 iterations.

Results of analyses performed with LHC and MC sampling are shown in Tables 8-10. Figs. 9-11 show results of analyses with LHC sampling technique in graphical format.

Analyses performed with MC sampling yielded similar probabilities and mean Fs values to those of LHC technique, but the computation time was drastically longer. The term "mean" safety factor value in Tables corresponds to the average value of Fs from all analyses.

Because of the negligible difference between the results of MC and LHC sampling techniques further analyses (that exclude the bond strength variability) are performed only for LHC evaluations. Results of these analyses are shown in Tables 11 and 12. As it can be concluded the bond strength is not the governing parameter as its variability doesn't have any influence on the analysis result.

Fig. 12 shows the variation of the safety factor value with the probability of failure for LHC sampling technique. This graph indicates that the probability of failure is highly dependent on the surface search technique, while the deterministic safety factor values are relatively consistent (refer to Table 7).

8. Discussion

Comprehensive slope stability analyses showed that the probability of failure is highly dependent on the chosen

Table 10 Mean factor of safety and reliability index with bond strength variability for different sampling and optimization techniques (normal distribution)

Fs(mean) / RI	Circular surfaces		Non-circular surfaces		
	Slope search	Auto Refine search	Path search	Cuckoo search	Particle swarm search
MC (5000 evaluations)	1.214 / 3.265	1.075 / 0.968	0.776 / -1.352	0.852 / -0.748	1.034 / 0.153
LHC (500 evaluations)	1.213 / 3.298	1.075 / 0.961	0.799 / -0.989	0.855 / -0.711	1.032 / 0.145

Table 11 Probability of failure without bond strength variability (for LHC 500 evaluations)

β / Normal distribution	Circular surfaces		Non-circular surfaces		
	Slope search	Auto Refine search	Path search	Cuckoo search	Particle swarm search
LHC	0.0 / 0.0	19.80 / 17.40	80.80 / 87.20	67.0 / 69.20	30.20 / 33.60
Computation time	4min / 4min	8h 32min / 8h 43min	6h 55min / 6h 43min	9h 44min / 9h 28min	9h 15min / 9h 02min

Table 12 Mean factor of safety and reliability index without bond strength variability (for LHC 500 evaluations)

Fs(mean) / RI	Circular surfaces		Non-circular surfaces		
	Slope search	Auto Refine search	Path search	Cuckoo search	Particle swarm search
β distribution	1.215 / 3.225	1.075 / 0.946	0.806 / -0.944	0.853 / -0.748	1.043 / 0.202
Normal distribution	1.213 / 3.298	1.075 / 0.961	0.802 / -0.934	0.845 / -0.745	1.023 / 0.101

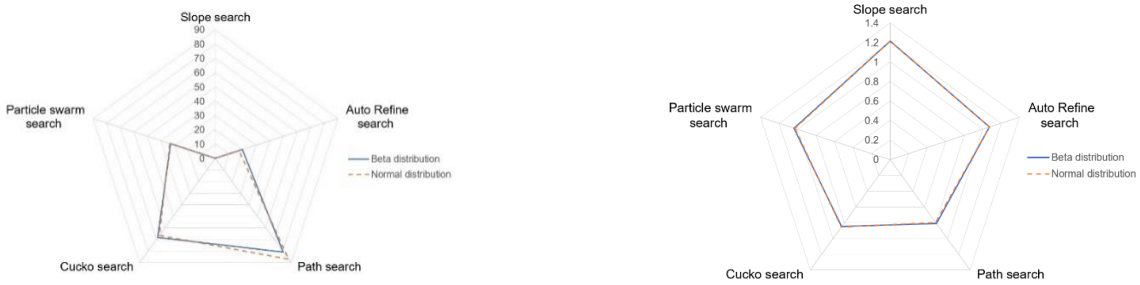

(a) Probability of failure (b) Mean factors of safety with respect to search

Fig. 11 Results of analyses with LHC sampling technique in the form of spider graphs

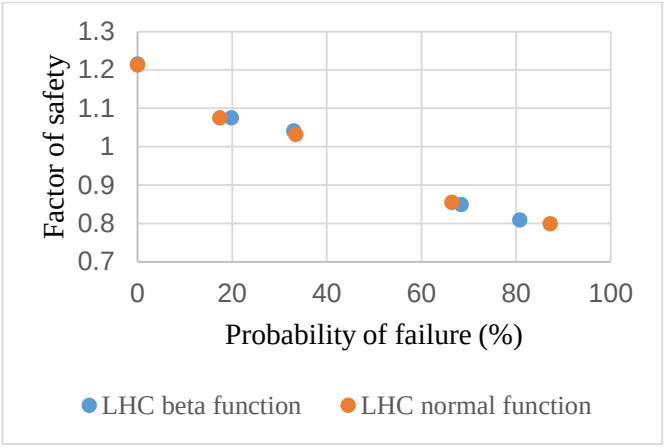

Fig. 12 Variation of P_f with mean F_s for different LHC optimization techniques (refer to Tables 8-10)

optimization search technique used to derive the results. In the analysed example probability of failure ranged between 0.0% (Slope circular search) and 87% (Path search).

Results of study by Wang *et al*. (2013) showed that the back-analysis of slope failure produced P_f=17.30%. This finding is consistent with the result of probabilistic analysis

considering Auto refine search (P_f=17.40 - 19.80%, depending on the choice of statistical distribution for input variables). Further on, if total length of the cut no. 2 (approx. 700 m) is divided by the failed portion of the slope (approx. 100 m) expected probability of failure equals P_f=14.28%.

For circular failure surface and slope search technique factors of safety for anisotropic case are Fs=1.204 (deterministic analysis) producing stable slope with P_f=0.0% (Tables 8 and 11). The background of this result is related to the relatively small variability of discontinuity shear strength parameters which, for the slope with the factor of safety higher than approx. Fs=1.2, produces stable solution in every probabilistic evaluation. The variation of deterministic safety factor values for other optimization techniques is small and acceptable from the practical point of view. Factors of safety vary between 1.013 and 1.103 (as summarized in Table 7). These analyses have proved that the slope was marginally stable at the time of completion.

Fig. 4(a) shows that the anchor force steadily increased over the period of one-year until the breakage of the anchors and subsequent slope failure occurred. Initial structural design didn't consider anisotropy of moderately jointed schist which produced apparently safe solution. So, what could have caused the failure? As a consequence of excavation, the shear strength of the small portion of critical joint set, at the bottom of the upper micropile row, was reduced due to softening over time. This phenomenon eventually led to the failure of already marginally stable slope. Figs. 4(a) and 4(b) also shows that the connection between precipitation and slope deformation does not exist. Also, it should be emphasized that the failure occurred during August 2018 after a very warm and dry summer.

Different types of statistical distributions of input parameters have very small influence on the analysis result, even though they produce different performance functions of the factor of safety (Figs. 9 and 10).

In this regard, the choice of probability distribution of input parameters is not as important as the choice of optimization technique. This statement cannot be accepted as a general conclusion in slope probabilistic analysis, thus it is relevant only for the analysed case. For example, Jiang *et al*. (2011) have shown that different probability distributions of shear strength parameters could influence the failure probability to a large extent. Due to this reason, it is important to ascribe proper PDF functions to input parameters prior to the probabilistic slope stability analysis. Large number of executed shear strength tests (laboratory or in situ) are the only proper indicator of soil/rock statistical strength variability.

Sampling techniques (LHC and MC) should yield similar results considering that the sufficient number of safety factor evaluations is chosen to achieve converged solution.

Probabilistic analyses are usually time consuming, depending on the number of realizations and optimization technique used to obtain the results, so the time necessary for the performance of each technique is emphasized (see Tables 8 and 11). The circular slope search technique (without additional optimization) is less time consuming compared to the others. For the same a priori assumptions the time needed to perform computation with slope search is between several and ten minutes. Analyses performed with other techniques usually take several hours. The non-circular search techniques, with additional optimization, took much more computational time than the circular search techniques. For example, computation time for Cuckoo search lasted approximately 11h and 30 min for LHC sampling (500 evaluations) and 23h and 30 min for MC sampling (5000 evaluations). Obtained results indicate that the preferable optimization technique does not exist for the analyzed reinforced rock slope, thus it is recommended to perform analyses by combining multiple optimization techniques to bring reasonable conclusions. There is no standardized procedure for choosing the proper optimization technique. This fact could be an obstacle for routine application of probabilistic concepts in everyday design.

For the analyzed case study, the variability of bond strength parameters does not influence the analysis results (see Tables 8-12 for comparison of relevant results with and without bond strength variability). The reason lies in the fact that bond strength is much higher than the characteristic breaking force of anchors even for the worst-case scenario. This was also validated on-site as the anchors at the moment of failure have broken within the unbonded zone (after the ultimate force reached the tensile strength of anchors).

9. Conclusions

This study analyses the global stability of anisotropic schist rock slope with reinforcement measures by means of probabilistic concepts. Statistical distributions are assigned to the parameters of the critical joint set and to the anchor bond strength. For the analysed *JRC* and *JCS* variables of the critical joint set the "U" and "bell-shaped" β-distributions should be used to describe their variability.

Two sets of probabilistic analyses were performed with the different types of statistical distributions of input parameters. For each scenario, multiple analyses were performed by varying sampling method (Monte-Carlo or Latin-Hypercube simulation technique) and failure surface search method (for circular surfaces: Slope search and Auto refine search; for non-circular surfaces with additional optimization: Path search, Cuckoo and Particle swarm search).

The probability of failure of the analysed reinforced rock slope is highly dependent on the chosen optimization search technique used to derive the results. Practicing engineers must have this in mind when dealing with probabilistic slope stability analysis.

As opposed to the generally accepted opinion that the choice of statistical distribution of input parameters affects the probability of failure, in this particular case the results show that the failure probability is practically insensitive to the chosen type of statistical distribution (beta or normal).

Different sampling techniques (LHC and MC) should yield similar results considering that the sufficient number

of safety factor evaluations is chosen to achieve converged solution.

The computation time for probabilistic approach is highly dependent on the number of Fs evaluations, sampling and optimization search technique used.

Having in mind the inconsistency of results with respect to the chosen optimization technique, the probabilistic slope stability analysis, for the analyzed case, should be used with extreme caution. The reason for this inconsistency lies in the fact that for the analyzed cross-section, with complex geometrical conditions, anisotropic rock mass behavior and abundant reinforcement measures, some optimization techniques render critical factors of safety that are lower than unity in majority of probabilistic realizations, while other techniques in majority of cases produce safety factor values slightly higher than one. In this way the probability of failure is either high or low for the search technique applied in the analysis. This could be considered as the general finding when considering the reliability of marginally stable slopes (with deterministic safety factor value slightly higher than unity).

Acknowledgments

This paper is funded by the Government of the Republic of Serbia (The Science Fund of the Republic of Serbia), as a part of Serbian Science and Diaspora Collaboration Program - project Rock slope stability - back analysis of failures along rock cuttings - ROCKSTAB (application number 6524757). Also, the Erasmus+ grant (EMADRID03) for the stay of Professor Svetlana Melentijević at the University of Belgrade is acknowledged.

References

Aladejare, A.E. and Akeju, V.O. (2020), "Design and sensitivity analysis of rock slope using Monte Carlo simulation", *Geotech. Geol. Eng*., **38**, 573-585. https://doi.org/10.1007/s10706-019-01048-z.

Babu, G.L. and Mukesh, M.D. (2004), "Effect of soil variability on reliability of soil slopes", *Geotechnique*, **54**, 335-337. https://doi.org/10.1680/geot.2004.54.5.335.

Barton, N. (1973), "Review of a new shear strength criterion for rock joints", *Eng. Geol.*, **7**, 287-332. https://doi.org/10.1016/0013-7952(73)90013-6.

Barton, N. (1976), "The shear strength of rock and rock joints", *Int. J. Rock. Mech. Min. Sci. Geomech. Abstr*, **13**(9), 255-279. https://doi.org/10.1016/0148-9062(76)90003-6.

Barton, N. and Choubey, V. (1977), "The shear strength of rock joints in theory and practice", *Rock. Mech.*, (**10**)1-2, 1-54. https://doi.org/10.1007/BF01261801.

Berisavljević, Z, Berisavljević, D. and Žugić, Ž. (2019), "Slope stability analysis of anisotropic rock masses with directional strength models", *Proceedings of the 8th Int. Conf. Geotechnical Aspects in Civil Engineering*, Vrnjačka Banja, November.

Berisavljević, D., Berisavljević, Z. and Melentijević, S. (2022), "The shear strength evaluation of rough and infilled joints and its indications for stability of rock cutting in schist rock mass", *Bull. Eng. Geol. Environ.*, **81**. https://doi.org/10.1007/s10064-022-02580-8.

Box, G.P. and Wilson, K.B. (1951), "On the Experimental Attainment of Optimum Conditions", *J. R. Stat. Soc.*, **13**(1), 1-45. https://doi.org/10.1111/j.2517-6161.1951.tb00067.x.

Chakraborty, R. and Dey, A. (2022), "Probabilistic slope stability analysis: state-of-the-art review and future prospects", *Innov. Infrastruct. Sol.*, **7**. https://doi.org/10.1007/s41062-022-00784-1.

Cho, S.E. (2007), "Effects of spatial variability of soil properties on slope stability", *Eng. Geol.*, **92**, 97-109. https://doi.org/10.1016/j.enggeo.2007.03.006.

Christian, J.T., Ladd, C.C. and Baecher, G.B. (1994), "Reliability applied to slope stability analysis", *J. Geotech. Eng.*, **120**(12). https://doi.org/10.1061/(ASCE)0733-9410(1994)120:12(2180)

Design code (2013), *EN 1537*, Execution of special geotechnical works. Ground anchors, CEN

Design code (2015), *BS 8081:2015+A2:2018*, Code of practice for grouted anchors, The British Standards Insitution.

Duncan, J.M. (2000), "Factors of safety and reliability in geotechnical engineering", *J. Geotech. Eng.*, **126**. https://doi.org/10.1061/(ASCE)1090-0241(2000)126:4(307)

El-Ramly, H., Morgenstern, N.R. and Cruden, D.M. (2002), "Probabilistic slope stability analysis for practice", *Can. Geotech. J*., **39**, 665-683. https://doi.org/10.1139/t02-034.

Fenton, G.A. and Griffiths, D.V. (2008), *Risk assessment in geotechnical engineering*, John Wiley & Sons: Hoboken, N.J.

Forrest, W.S. and Orr, T.L. (2010), "Reliability of shallow foundations designed to Eurocode 7", *Georisk*, **4**(4), 186-207. https://doi.org/10.1080/17499511003646484.

Gholampour, A. and Johari, A. (2019), "Reliability-based analysis of braced excavation in unsaturated soils considering conditional spatial variability", *Comput. Geotech.*, **115**. https://doi.org/10.1016/j.compgeo.2019.103163.

Greco, V.R. (1996), "Efficient Monte Carlo technique for locating critical slip surface", *J. Geotech. Eng.*, **122**(7), 517-525. https://doi.org/10.1061/(ASCE)0733-9410(1996)122:7(517).

Griffiths D.V. and Fenton G.A. (2004), "Probabilistic slope stability analysis by finite elements", *J. Geotech. Geoenviron. Eng.*, **130**(5), 507-518. https://doi.org/10.1061/(ASCE)1090-0241(2004)130:5(507).

Guo, X., Sun, Q., Dias, D. and Antoinet, E. (2020), "Probabilistic assessment of an earth dam stability design using the adaptive polynomial chaos expansion", *Bull. Eng. Geol. Environ*., **79**, 4639-4655. https://doi.org/10.1007/s10064-020-01847-2.

Harr, M.E. (1987), *Reliability-based design in civil engineering* McGraw-Hill Inc., New York.

Hassan, A.M. and Wolff, T.F. (1999), "Search algorithm for minimum reliability index of earth slopes", *J. Geotech. Eng.,* **125**(4), https://doi.org/10.1061/(ASCE)1090-0241(1999)125:4(301).

Hoek, E. and Brown, E.T. (2019), "The Hoek–Brown failure criterion and GSI - 2018 edition", *J. Rock Mech. Geotech. Eng.*, **11**(3), 445-463. https://doi.org/10.1016/j.jrmge.2018.08.001.

Hoek, E., Carranza-Torres, C. and Corkum, B. (2002), "Hoek-Brown criterion-2002 edition", *Proceedings of the NARMS-TAC conference*, Toronto, July.

Huang, J., Griffiths, D.V. and Fenton, G.A. (2010), "System reliability of slopes by RFEM", *Soils Found.*, **50**(3), 343-353. https://doi.org/10.3208/sandf.50.343.

Javankhoshdel, S. and Bathurst, R.J. (2016), "Influence of cross correlation between soil parameters on probability of failure of simple cohesive and c-ϕ slopes", *Can. Geotech. J.*, **53**(5), 839-853. https://doi.org/10.1139/cgj-2015-0109.

Javankhoshdel, S. and Bathurst, R.J. (2014), "Simplified probabilistic slope stability design charts for cohesive and c-φ soils", *Can. Geotech. J*., **51**(9), 1033-1045. https://doi.org/10.1139/cgj-2014-0418.

Javankhoshdel, S., Cami, B., Yacoub, T. and Bathurst R.J. (2019),

"Probabilistic analysis of an MSE wall considering spatial variability of soil properties", *Proceedings of the 8th Int. Conf. on Case Histories in Geotechnical Engineering*, Philadelphia, March.

Javankhoshdel, S., Luo, N. and Bathurst, R.J. (2017), "Probabilistic analysis of simple slopes with cohesive soil strength using RLEM and RFEM", *Georisk*, **11**(3), 231-246. https://doi.org/10.1080/17499518.2016.12357122.

Javankhoshdel, S., Cami, B., Mafi, R., Yacoub, T. and Bathurst, R. J. (2018), "Optimization techniques in non-circular probabilistic slope stability analysis considering spatial variability", *Proceedings of the: GeoEdmonton 2018*, Edmonton, Canada.

Ji, J., Liao, H.J. and Low, B.K. (2012), "Modeling 2D spatial variation in slope reliability analysis using interpolated autocorrelations", *Comput. Geotech.,* **40**, 135-146. https://doi.org/10.1016/j.compgeo.2011.11.002.

Jiang, T., Liu, J., Yuan, B. and Wang, S. (2011), "Influence of probability distribution of shear strength parameters on reliability-based rock slope analysis", *Proceedings of the GeoHunan2011*, https://doi.org/10.1061/47627(406)9.

Johari, A. and Gholampour, A. (2018), "A practical approach for reliability analysis of unsaturated slope by conditional random finite element method", *Comput. Geotech.,* **102**, 79-91. https://doi.org/10.1016/j.compgeo.2018.06.004.

Johari, A., Fazeli, A. and Javadi, A.A. (2013), "An investigation into application of jointly distributed random variables method in reliability assessment of rock slope stability", *Comput. Geotech.*, **47**, 42-47. https://doi.org/10.1016/j.compgeo.2012.07.003.

Johari, A., Hajivand, A.K. and Binesh, S. (2020), "System reliability analysis of soil nail wall using random finite element method", *Bull. Eng. Geol. Environ.*, **79**, 2777-2798. https://doi.org/10.1007/s10064-020-01740-y.

Kim, H.Y. (2013), "Statistical notes for clinical researchers: assessing normal distribution (2) using skewness and kurtosis", *Restor. Dent. Endod*., **38**(1), 52-54. https://doi.org/10.5395/rde.2013.38.1.52.

Kitch, W.A. (1994), "Deterministic and probabilistic based analyses of reinforced soil slopes", PhD Dissertation, University of Texas at Austin

Kulhawy, F.H., Roth, M.J. and Grigoriu, M.D. (1991), "Some statistical evaluations of geotechnical properties", *Proceedings of the 6th Int. Conf. on Applications of Statistics and Probability in Soil and Structural Engineering*, Mexico City, June.

Lacasse, S. and Nadim, F. (1996), "Uncertainties in characterizing soil properties", *Proceedings of the Uncertainty in the Geologic Environment: From Theory to Practice,* New York, July – August.

Law, A.M. and McComas, M.G. (1986), "Pitfalls in the simulation of manufacturing systems", *Proc. Winter Simulation Conference*, Washington, D.C, December.

Li, K.S. and Lumb, P. (1987), "Probabilistic design of slopes", *Can. Geotech. J.*, **24**, 520-535. https://doi.org/10.1139/t87-06.

Li, S., Shangguan, Z., Duan, H., Liu, Y. and Luan, M. (2009), "Searching for critical failure surface in slope stability analysis by using hybrid genetic algorithm", *Geomech. Eng*., **1**(1), 85-96. https://doi.org/10.12989/gae.2009.1.1.085.

Li, J., Zhang, S., Liu, L., Wu, J. and Cheng, Y. (2022), "Adaptively selected autocorrelation structure-based Kriging metamodel for slope reliability analysis", *Geomech. Eng.*, **30**(2), 187-199. https://doi.org/10.12989/gae.2022.30.2.187.

Li, D.Q., Zhou, C.B., Lu, W.B. and Jiang, Q.H. (2009), "A system reliability approach for evaluating stability of rock wedges with correlated failure modes", *Comput. Geotech.*, **36**(8) , 1298-1307. https://doi.org/10.1016/j.compgeo.2009.05.013.

Low, B.K., Gilbert, R.B. and Wright, S.G. (1998), "Slope reliability analysis using generalized method of slices", *J. Geotech. Geoenviron. Eng*., **124**(4), 350-362. https://doi.org/10.1061/(ASCE)1090-0241(1998)124:4(350).

Low, B.K., Lacasse, S. and Nadim, F. (2007), "Slope reliability analysis accounting for spatial variation", *Georisk*, **1**(4), 177-189. https://doi.org/10.1080/17499510701772089.

Lumb, P. (1966), "The variability of natural soils", *Can. Geotech. J*., **3**(2), 74-97. https://doi.org/10.1139/t66-009.

Lumb, P. (1970), "Safety factors and the probability distribution of soil strength", *Can. Geotech. J.*, **7**(3), 225-242. https://doi.org/10.1139/t70-032.

McKay, M.D., Beckman, R.J. and Conover, W.J. (1979), "A comparison of three methods for selecting values of input variables in the analysis of output from a computer code", *Technometrics*, **21**(2), 239-245. https://doi.org/10.2307/1268522.

Mostyn, G.R. and Li, K.S. (1993), "Probabilistic slope stability analysis - state-of-play" (Chapter), *Probabilistic methods in geotechnical engineering*, Balkema, Rotterdam.

Nguyen, V.U. and Chowdhury, R.N. (1985), "Simulation for risk analysis with correlated variables", *Géotechnique*, **35**(1), 47-58. https://doi.org/10.1680/geot.1985.35.1.47.

Pearson, K. (1916), "Mathematical contributions to the theory of evolution, XIX: Second supplement to a memoir on skew variation", *Philos. T. Roy. Soc. A*, **216**(538-548), 429-457. https://doi.org/10.1098/rsta.1916.0009.

Shapiro, S.S. and Wilk, M.B. (1965), "An analysis of variance test for normality (complete samples)", *Biometrika*, **52**(3-4), 591-611. https://doi.org/10.1093/biomet/52.3-4.591.

Rafiei Renani, H., Martin, C.D., Varona, P. and Lorig, L. (2019), "Stability Analysis of Slopes with Spatially Variable Strength Properties" *Rock. Mech. Rock. Eng.,* **52**, 3791-3808. https://doi.org/10.1007/s00603-019-01828-2.

Rafiei Renani H. and Martin, C.D. (2020), "Slope stability analysis using equivalent Mohr-Coulonb and Hoek-Brown criteria", *Rock Mech. Rock Eng*., **53**(13-21). https://doi.org/10.1007/s00603-019-01889-3.

GuhaRay, A. and Baidya, D.K. (2014), "Partial safety factors for retaining walls and slopes: A reliability based approach", *Geomech. Eng.*, **6**(2), 99-115. https://doi.org/10.12989/gae.2014.6.2.099.

Rétháti, L. (1988), *Probabilistic Solutions in Geotechnics*, Elsevier

Robert, C.P. and Casella, G. (2004), *Monte Carlo Statistical Methods*, Springer, Berlin.

Rocscience (2021), "Slide2 2D Limit Equilibrium Analysis for Slopes" version 9.020. https://www.rocscience.com.

Rocscience (2022), "Slide2 online user guide", https://www.rocscience.com/help/slide2/documentation.

Spencer, E.E. (1967) "A method of the analysis of the stability of embankments assuming parallel inter-slice forces", *Géotechnique*, **17**, 11-26. https://doi.org/10.1680/geot.1967.17.1.11.

Tietje, O., Fitze, P. and Schneider, H.R. (2014), "Slope stability analysis based on autocorrelated shear strength parameters", *Geotech. Geol. Eng.*, **32**, 1477-1483. https://doi.org/10.1007/s10706-013-9693-8.

US Army Corps of Engineers (1997), Engineering and Design: Introduction to Probability and Reliability Methods for use in Geotechnical Engineering (Technical Letter), Washington DC.

Wang, L., Hwang, J.H., Luo, Z., Juang, C.H. and Xiaoz, J. (2013), "Probabilistic back analysis of slope failure - A case study in Taiwan", *Comput. Geotech.*, **51**, 12-23. https://doi.org/10.1016/j.compgeo.2013.01.008.

Wang, L., Wu, C., Gu, X., Liu, H., Mei, G. and Zhang, W. (2020), "Probabilistic stability analysis of earth dam slope under transient seepage using multivariate adaptive regression splines", *Bull. Eng. Geol. Environ*., **79**, 2763-2775 https://doi.org/10.1007/s10064-020-01730-0.

Wang, L., Wu, C., Tang, L., Zhang, W., Lacasse, S., Liu, H. and Gao, L. (2020), "Efficient reliability analysis of earth dam slope stability using extreme gradient boosting method", *Acta Geotech.*, **15**, 3135-3150. https://doi.org/10.1007/s11440-020-00962-4.

Wolf, T.F. (1996), "Probabilistic slope stability in theory and practice", *Uncertainty in the Geologic Environment: from Theory to Practice*, ASCE.

Wu, T.H. and Kraft, L.M. (1970), "Safety analysis of slopes", *J. Soil Mech. And Found. Div.*, **96**(2), 609-630. https://doi.org/10.1061/JSFEAQ.0001406.

Yang, X.L. and Liu, Z.A. (2018), "Reliability analysis of three-dimensional rock slope", *Geomech. Eng.*, **15**(6), 1183-1191. https://doi.org/10.12989/gae.2018.15.6.1183.

Yucemen, M.S., Tang, W.H. and Ang, A.S. (1973), A Probabilistic Study of Safety and Design of Earth Slopes (Technical Report), University of Illinois at Urbana-Champaign

Zhang, J., Tang, W.H. and Zhang, L. (2010), "Efficient probabilistic back-analysis of slope stability model parameters", *J. Geotech. Geoenviron. Eng.*, **136**, 99-109. https://doi.org/10.1061/(ASCE)GT.1943-5606.0000205.

Zhang, W., Gu, X., Hong, L., Han, L. and Wang, L. (2023), "Comprehensive review of machine learning in geotechnical reliability analysis: Algorithms, applications and further challenges", *Appl. Soft Comput.*, **136**. https://doi.org/10.1016/j.asoc.2023.110066

Zhao, L., Jiao, K., Zuo, S., Yu, C. and Tang., G. (2020), "Pseudo-static stability analysis of wedges based on the nonlinear Barton-Bandis failure criterion", *Geomech. Eng.,* **20**(4), 287-297. https://doi.org/10.12989/gae.2020.20.4.287.

Zhou, X., Chen, J., Chen, Y. et al. (2017) "Bayesian-based probabilistic kinematic analysis of discontinuity-controlled rock slope instabilities", *Bull. Eng. Geol Environ*., **76**, 1249-1262. https://doi.org/10.1007/s10064-016-0972-5

CC